Spectrochimica Acta Part A: Molecular and Biomolecular Spectroscopy 287 (2023) 122062

Contents lists available at ScienceDirect

Spectrochimica Acta Part A: Molecular and Biomolecular Spectroscopy

journal homepage: www.journals.elsevier.com/spectrochimica-acta-part-a-molecular-and-biomolecular-spectroscopy

Use of polymers as wavenumber calibration standards in deep-UVRR

Aikaterini Pistiki [a], Oleg Ryabchykov [a,c], Thomas W. Bocklitz [a,c], Petra Rösch [b,c,*], Jürgen Popp [a,b,c,d,e]

[a] Leibniz Institute of Photonic Technology Jena, Albert-Einstein-Str. 9, 07745 Jena, Germany
[b] InfectoGnostics Research Campus Jena, Philosophenweg 7, 07743 Jena, Germany
[c] Institute of Physical Chemistry and Abbe Center of Photonics, Friedrich Schiller University, Lessingstraße 10, 07743 Jena, Germany
[d] Jena Biophotonics and Imaging Laboratory, Albert-Einstein-Str. 9, 07745 Jena, Germany
[e] Center for Sepsis Control and Care, Jena University Hospital, Am Klinikum 1, 07747 Jena, Germany

HIGHLIGHTS

- Deep-UVRR needs to be standardized when developed for clinical diagnostics.
- Wavenumber calibration is important for this attempt.
- PEI, PET, PS and Teflon are suitable for wavenumber calibration in deep-UVRR.
- PET and Teflon perform best in the classification of Gram-positive pathogens.
- Discrimination of *Enterobacteriaceae* is challenging independent of the used polymer.

GRAPHICAL ABSTRACT

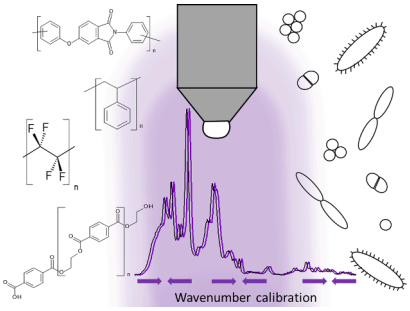

ARTICLE INFO

Keywords:
Deep-UV resonance Raman spectroscopy
Wavenumber calibration
Polymers
Bacterial species differentiation

ABSTRACT

Deep-UV resonance Raman spectroscopy (UVRR) allows the classification of bacterial species with high accuracy and is a promising tool to be developed for clinical application. For this attempt, the optimization of the wavenumber calibration is required to correct the overtime changes of the Raman setup. In the present study, different polymers were investigated as potential calibration agents. The ones with many sharp bands within the spectral range 400–1900 cm^{-1} were selected and used for wavenumber calibration of bacterial spectra. Classification models were built using a training cross-validation dataset that was then evaluated with an independent test dataset obtained after 4 months. Without calibration, the training cross-validation dataset provided an accuracy for differentiation above 99 % that dropped to 51.2 % after test evaluation. Applying the test evaluation with PET and Teflon calibration allowed correct assignment of all spectra of Gram-positive isolates. Calibration with PS and PEI leads to misclassifications that could be overcome with majority voting. Concerning the very closely related and similar in genome and cell biochemistry *Enterobacteriaceae* species, all spectra of the training cross-validation dataset were correctly classified but were misclassified in test evaluation. These results show the importance of selecting the most suitable calibration agent in the classification of bacterial species and help in the optimization of the deep-UVRR technique.

* Corresponding author at: Institute of Physical Chemistry and Abbe Center of Photonics, Friedrich Schiller University, Lessingstraße 10, 07743 Jena, Germany.
E-mail address: petra.roesch@uni-jena.de (P. Rösch).

https://doi.org/10.1016/j.saa.2022.122062
Received 27 June 2022; Received in revised form 10 October 2022; Accepted 29 October 2022
Available online 2 November 2022

1. Introduction

Raman spectroscopy is a sensitive, rapid and label-free analytical technique that has found application in biological science over the past decades. In bacterial samples, unique spectra can be obtained by detecting vibrational modes of the chemical bonds in their macromolecules, containing information on the biochemical composition of the bacterial cells [1–5]. The minimal required sample preparation, the high analysis speed and the low analysis cost due to the absence of expensive consumables make Raman spectroscopy a very promising analytical tool for clinical microbiology [6].

In deep-UV resonance Raman spectroscopy (UVRR) mostly molecules with an aromatic ring in their chemical structure are in resonance. This results in a large increase of the signal from these molecules that dominate the spectrum. When applying this technique to bacterial samples the acquired spectrum consists mainly of Raman bands from nucleic acid and aromatic amino acids, allowing a selective spectroscopic analysis of these molecules [7,8]. This simplifies the analysis profile, allowing discrimination on genus, species, or even strain level [6]. This advantage of deep-UVRR has been previously shown to enable the classification of many bacterial species [9], including clinical isolates [10] making it an attractive tool for clinical application.

For the development of a robust and reliable clinical tool, the regulatory authorities require the validation of the technique [11,12]. In Raman spectroscopy, wavenumber calibration is an important factor in this attempt since the overtime shift of the Raman setup requires constant correction during chemometric analysis. In addition, the spectral influence of the Raman setup needs to be removed to obtain comparable results. This is of higher importance in large datasets and databases obtained over an extensive time periode, especially when the identification of unknown samples is aimed [13]. In deep-UVRR, the selection of a suitable wavenumber calibration agent is challenging due to the occurring photodegradation when exposed to such low wavelengths. Over the years many different substances have been used for wavenumber calibration in deep-UVRR including polymers [14–16], diamond crystals [17], ethanol [18], or even the O_2 and N_2 stretching vibration bands of air [7]. However, many of these agents perform poorly since their spectra contain of only a few sharp bands covering just partly the required spectral range and are therefore not suitable for the optimization of deep-UVRR for clinical application. In addition, to our knowledge, no standard procedure exists as well as no systematic investigation on the most suitable calibration agents has been performed so far for deep-UVRR.

Another mandatory factor for the application of Raman spectroscopy in clinical microbiology is the requirement for reliable differentiation of clinical isolates including the large group *Enterobacteriaceae*. This is a group of evolutionary closely related and very similar bacteria that includes common human pathogens such as *Escherichia coli* and *Klebsiella* spp. [19]. Deep-UVRR has been shown to be a promising tool in this attempt since it allowed the differentiation of *Escherichia coli* and *Klebsiella* spp. clinical isolates, as well as the differentiation of *Klebsiella pneumoniae* and *Klebsiella oxytoca* strains with high accuracy [20]. These results indicate the applicability of deep-UVRR in clinical microbiology and its potential to be developed into a routinely used, diagnostic tool for clinical diagnostics of infectious diseases. For this attempt, a standardization of the method is required that also includes appropriate wavenumber calibration.

In the present study, it is aimed to investigate for the first time the suitability of different polymers as calibration agents for deep-UVRR and evaluate their performance in differentiating clinical isolated bacterial species, including *Enterobacteriaceae*. For this attempt, different polymers were selected based on their chemical structure and tested.

2. Materials and methods

2.1. Polymers

Nine different Polymers were chosen for this study based on their chemical structure: Polysulfone (PSU), Polyether ether ketone (PEEK), Polyphenylene sulfide (PPS) and Polyetherimide (PEI) were provided by Gebr. DOLLE GmbH (Bad Köstritz, Germany). Teflon was purchased from TECHNOPLAST v.TRESKOW GMBH, Germany. For the Polyethylene terephthalate (PET) polymer a transparent packing made of PET was used, for the Polyurethane (PU) polymer a sponge was used purchased from a local supermarket, for the melamine resin a coated MDF plate was used and for the Polystyrene (PS) a petri dish (Sarstedt, Germany) was used. The chemical structures of the used polymers are shown in Fig. 1. The chemical structure of all polymers except Teflon and PU contain aromatic rings that can generate a resonance effect in deep UVRR.

2.2. Deep-UVRR

For the collection of the UV resonance Raman spectra, a Raman setup (HR800, Horiba/Jobin-Yvon) with a focal length of 800 mm coupled with an argon-ion laser (Coherent Innova 300, FReD) was used. The frequency of the 488 nm line was doubled to produce a wavelength of 244 nm. The laser was directed and focused on the sample through an × 20 antireflection-coated objective (LMU, NA: 0.5, UVB). Backscattered Raman light was collected through a 400 μm entrance slit into a 2400 lines/mm grating and detected by a nitrogen-cooled CCD camera leading to a spectral resolution of 2 cm^{-1}. To avoid burning the samples, the sample stage was constantly rotated in a spiral manner during measurement.

The polymers were placed under the Raman microscope and two consecutive spectra were collected using an integration time of 30 s each. The two spectra were then averaged. This was repeated five times for each polymer and replicate (batch).

2.3. Bacteria sample preparation

The bacteria were freshly cultured from frozen stock onto nutrient agar (NA) plates for every measurement day. To avoid intrasample variations related to the different growth stages of the bacteria on the plates, 2–3 loopful of biomass were transferred from the agar plate into 20 ml Nutrient Broth (NB) (Carl Roth) and incubated for 1 h in a shaking incubator at 37 °C and 120 rpm to reach the exponential phase. 1.5 ml of the inoculum was transferred into two separate Eppendorf tubes and was heat inactivated at 99 °C, the Gram-negative bacteria for 5 min and the Gram-positive bacteria were inactivated for 10 min. Afterward, 3 consecutive washings with 1 ml deionized water (DI) using centrifugation at 5000 g for 5 min (Rotina 380R, Hettich) [21,22] were performed and the bacterial pellets were then resuspended in 30 μl DI. Each replicate was placed onto a fused-silica slide (B&M Optik GmbH, Germany) to air dry at room temperature for ~ 1 h. To verify the heat-inactivation, bacteria were plated onto NA plates, incubated for 24 h at 37 °C and no growth could be detected. Each Raman measurement consisted of 10 consecutive measurements of 15 s integration that were afterward averaged to reduce noise. A total of four biological replicates (batches) were measured for each strain on different days. Each batch for each bacterial species consisted of 20 measurements collected from 2 fused silica slides to avoid remeasuring burned areas of the sample and a total of 200 spectra per isolate and batch were collected.

2.4. FT-Raman

Polymers were measured using a Multispec Fourier-transform Raman-Spectrometer (Bruker Corporation, Billerica, USA) coupled with a 1064 nm Nd: YAG laser (Klastech DeniCAFC-LC-3/40, Dortmund,

Germany). A laser power of 1000 mW was used. To achieve peak positions that were as precise as possible, a spectral resolution of 0.7 cm^{-1} was used. 256 accumulations were recorded and were afterward averaged to improve the signal-to-noise ratio.

2.5. Data analysis

Preprocessing and data analysis were done using the RAMANMETRIX software (https://ramanmetrix.eu) [23]. Prior to analysis, several preprocessed steps were performed.

The deep-UVRR and FT-Raman spectra from the different polymers were de-spiked with a manual threshold as previously described by Ryabchykov *et al.* [24], interpolated on the linear wavenumber axis with a step of 1 cm^{-1}, baseline corrected using a Sensitive Nonlinear Iterative Peak (SNIP) clipping algorithm with 40 iterations followed by vector normalization. Spectra were then truncated to the relevant range of 500–1900 cm^{-1}. FT-Raman spectra were afterward plotted in Origin 2018b software and the precise peak-positions were defined with a peak-fitting function using the Voigt profile. These band positions were then used as "reference standards" for the polymer spectra measured with the deep-UVRR.

The pre-processing of the bacteria spectra included the same despiking procedure as described above. Afterward, spectra were wavenumber calibrated using the 4 polymers that were selected to be suitable. The shift in the polymer spectra was corrected using "reference standards" peak positions from the FT-Raman spectra. Calibration was performed using a spline peak fitting method. Because some substances had a low number of peaks, a linear calibration function was utilized. Spectra were afterward interpolated on the linear wavenumber axis, baseline corrected, and vector normalized as described above.

To validate the data quality in training cross-validation and independent test evaluation datasets, the signal-to-noise ratio (SNR) was calculated by dividing the mean of the median smoothed spectrum with a window size of 5 by the standard deviation of noise. The noise was estimated as the difference between the original and the smoothed spectrum.

2.6. Classification models of bacteria calibrated with the different polymers

Five different classification models were built, four using the wavenumber calibrated data with the selected polymers as calibration standard and one without calibration that was used as control. For the classification of the bacterial strains, PCA-LDA models with a leave-one-batch-out cross-validation (LOBOCV) were trained using the training cross-validation dataset that consisted of 3 batches representing 3 measurement days. The optimal number of principal components (PC) was selected automatically based on the LOBOCV, limited to a maximum of 10 PCs. The independent test dataset, consisting of 1 batch, that was measured after 4 months, was then used for the final evaluation. Majority voting was applied to reduce intra-sample heterogeneity in the bacteria spectra. Finally, spectra were visualized using Origin (Pro), version 2018b (OriginLab Corporation, Northampton, USA).

3. Results

As a first step, 9 different polymers were tested on their suitability to be used as calibration agents in deep-UVRR. Spectra from all used polymers are shown in Fig. 2. It can be seen that the polymers in Fig. 2A do not display many sharp and clearly defined bands within the spectral range and were therefore excluded from further analysis as unsuitable calibration agents. The polymers in Fig. 2B however, show distinct sharp bands in most of the required spectral range and were considered suitable for wavenumber calibration since they should allow interpolation and extrapolation of the Raman band positions in the bacterial spectra. PEEK was excluded from further analysis due to the not well-resolved double peak around 1600 cm^{-1} as well as the absence of sharp bands below 800 cm^{-1}. UV–vis absorption spectra of the polymers of Fig. 2B are shown in supplementary figure S1.

To define the exact band positions of the selected polymers, FT-Raman spectra were obtained and used as "reference standards" for the polymer spectra measured with the deep-UVRR. In Fig. 3 the single FT-Raman spectra of the 4 chosen polymers are shown in comparison to the average deep-UVRR spectra of the training data. It can be seen that most bands present in the FT-Raman spectra are also present in the deep-UVRR spectra of the polymers. Since FT-Raman spectroscopy offers the advantage in the determination of the Raman-band position with high

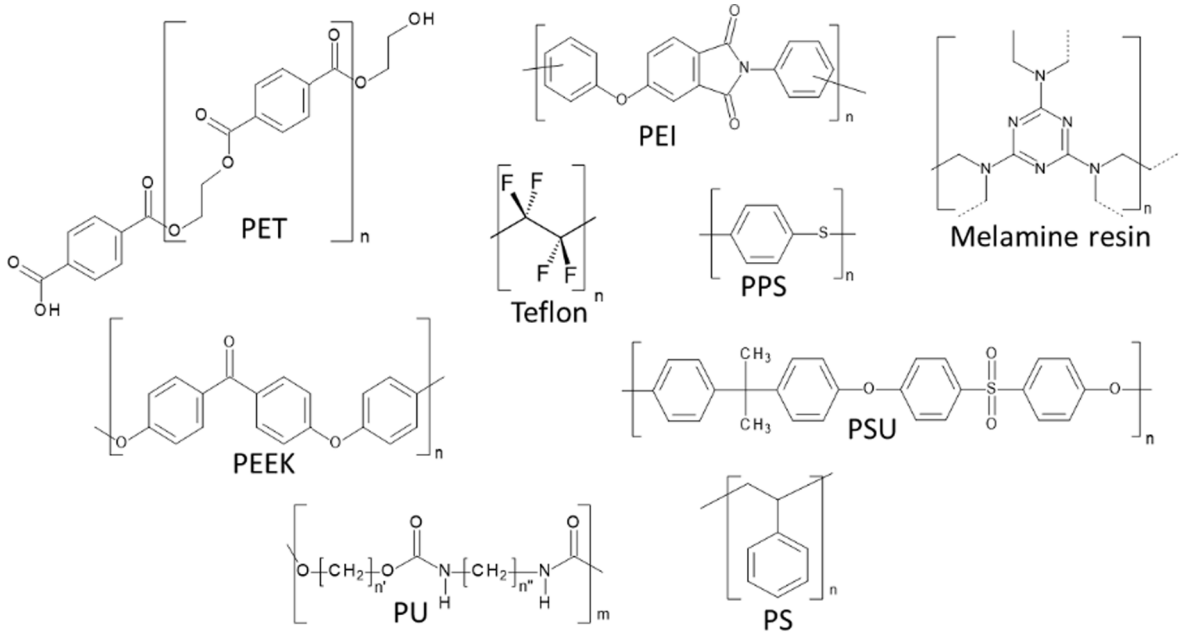

Fig. 1. Chemical structure of the used polymers.

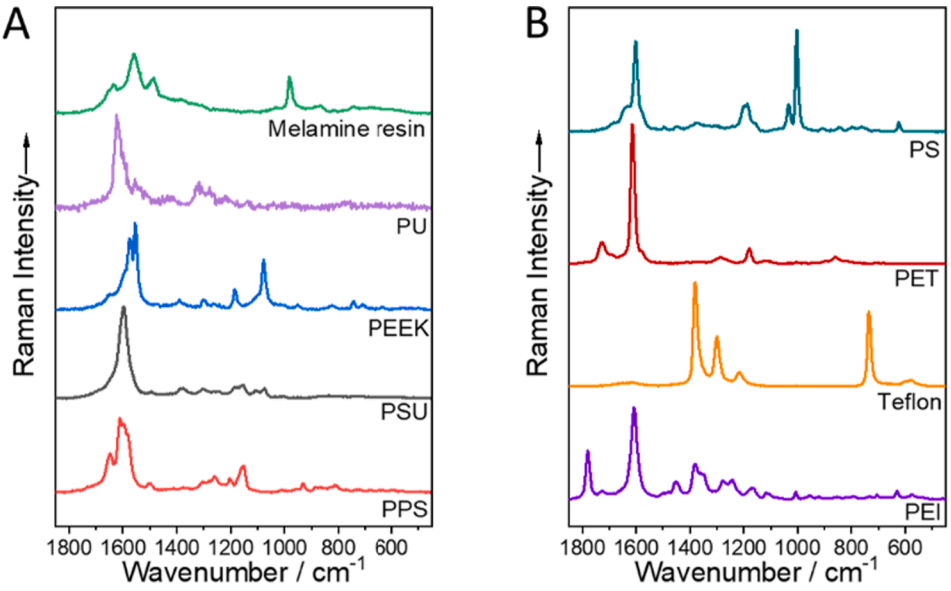

Fig. 2. Deep-UVRR spectra of potential polymers for wavenumber calibration.

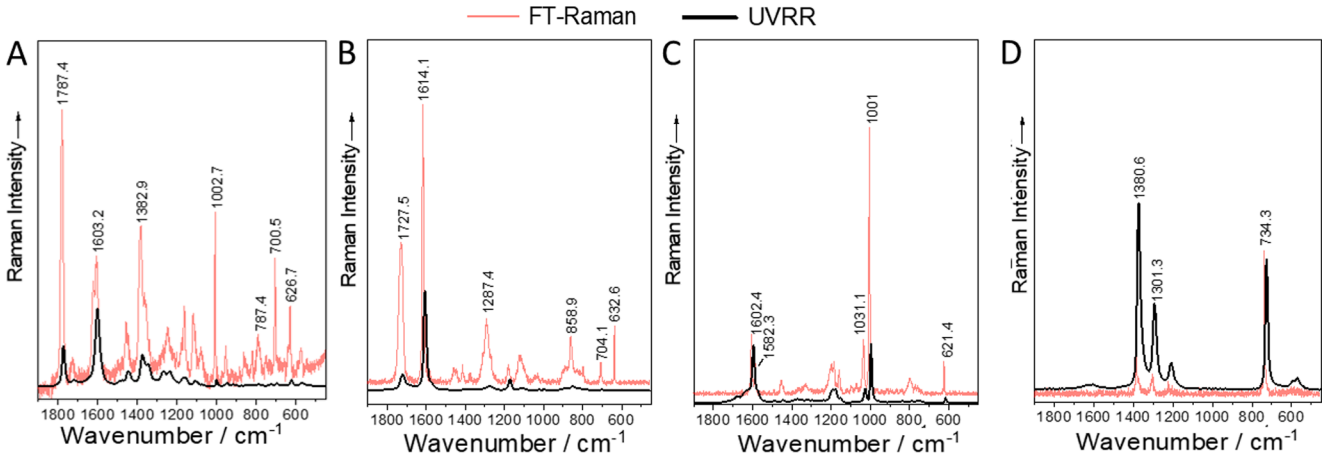

Fig. 3. FT-Raman and deep-UVRR spectra of the training cross-validation dataset from the selected polymers. A. PEI, B. PET, C. PS and D. Teflon.

precision, these band positions can be used as reference standards for the deep-UVRR spectra.

Using the selected polymers as calibration agents, classification models were trained for the differentiation of clinical isolates of 4 bacterial species, including strains from the *Enterobacteriaceae* group. These models were then finally evaluated using an independent test dataset, measured 4 months later. To assess the performance of the different calibration agents, the results of the models were compared to a model built without wavenumber calibration of the spectra ("uncalibrated spectra"). In Fig. 4 uncalibrated bacteria spectra from the training cross-validation dataset are shown. In Table 1 the sensitivities of the classification results of the bacterial species for the training data cross-validation and the predictions of the independent test evaluation dataset are shown. Detailed classification results can be seen in supplementary tables S1-S5. For uncalibrated spectra, in the training cross-validation dataset the model performance yielded an accuracy above 99 %, indicating a nearly perfect classification of the individual spectra of each bacterial species. Only one spectrum was misclassified between *Escherichia coli* and *Klebsiella pneumoniae*, two closely related, Gram-negative *Enterobacteriaceae* species with high similarities in their biochemical composition. It is interesting to observe that, despite the high similarities present in these two species, the model could

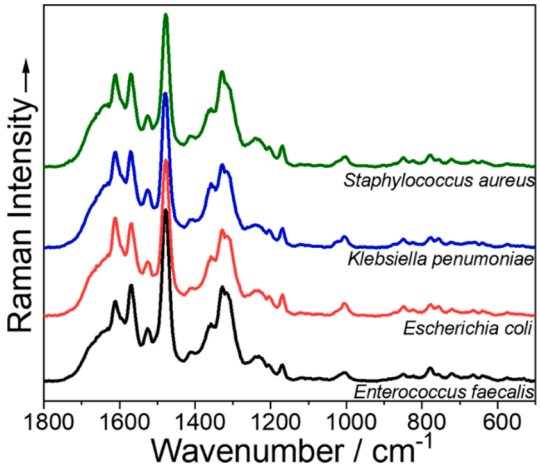

Fig. 4. Uncalibrated Deep-UVRR bacteria spectra.

Table 1
Sensitivities of classification results for each bacterial species for the training cross-validation and the prediction of test data for the different calibration treatments.

	Uncalibrated		PEI		PET		PS		Teflon	
	Cross-validation (%)	Test (%)	Cross-validation (%)	Test (%)	Cross-validation (%)	Test (%)	Cross-validation (%)	Test (%)	Cross-validation (%)	Test (%)
Enterococcus faecalis	100	50	100	55	100	100	100	55	100	100
Escherichia coli	100	50	100	100	89.8	100	100	100	100	100
Klebsiella pneumoniae	98.3	50	98.3	0	98.3	5	98.3	0	98.3	0
Staphylococcus aureus	100	50	100	100	100	100	100	100	100	100
Accuracy	**99.6**	**51.2**	**99.6**	**64.6**	**97.1**	**76.8**	**99.6**	**64.6**	**99.6**	**75.6**

distinguish them with high performance. This, however, changes dramatically when test-evaluating with an independent dataset that was measured after 4 months. The accuracy of the model drops from 99.6 to 51.2 %, with all spectra from 2 of the 4 species being classified incorrectly. It can be seen that in the test data the model is incapable to distinguish between the two *Enterobacteriaceae* species, classifying all *Klebsiella pneumoniae* spectra as *Escherichia coli*. In addition, the model is also not able to distinguish between the two Gram-positive species, classifying all spectra of *Enterococcus faecalis* as *Staphylococcus aureus*. This indicates that the overtime shift of the device significantly changes the spectra not allowing the model to correctly identify the fine differences between species leading to a decrease in its performance by differentiating only the Gram-positive from Gram-negative isolates. Mean spectra of the training cross-validation and test evaluation dataset for each bacterial species are shown in Supplementary Figures S2-S5. The most important Raman bands of the spectra are marked with lines and it can be seen that in the training dataset no wavenumber shifts occur after calibration with all polymers compared to the uncalibrated spectra. This happens due to the absence of overtime shift of the device within the 3 days in which this dataset was obtained.

The differences between the original and calibrated wavenumber axis for each polymer of both the training and validation datasets are shown in Supplementary Figure S6. For all used calibration agents, the performance of the model using the training cross-validation dataset is above 97 % indicating nearly perfect differentiation of the spectra from each bacterial species, similar to when no calibration is performed. The few misclassifications, 7 when calibrating with PET and 1 in all other polymers, are again only between *Escherichia coli* and *Klebsiella pneumoniae*, with all spectra of the two Gram-positive isolates being classified correctly. After test evaluation, higher accuracies can be observed for all calibration agents compared to no-calibration and only small wavenumber shifts are present in the mean spectra of all bacteria species after calibration with the different polymers (Figures S2-S5), as it can be seen when following the dashed lines. However, none of the calibration agents could improve the model's performance in differentiating the *Enterobacteriaceae* species, where again almost all *Klebsiella pneumoniae* spectra were misclassified as *Escherichia coli*. Concerning the Gram-positive isolates, the calibration with PET and Teflon could provide a correct classification of all spectra, whereas for PEI and PS 9 out of 20 *Enterococcus faecalis* spectra were incorrectly classified as *Staphylococcus aureus*. Despite these misclassifications, the majority of the spectra were still correctly classified, allowing correct identification of the species when applying majority voting, as shown in Tables 2 and S6.

Table 2
Sensitivities of classification results for each bacterial species after test evaluation and majority voting, when PEI and PS were used as calibration agents.

	PEI	PS
	Predicted (%)	Predicted (%)
Enterococcus faecalis	100	100
Escherichia coli	100	100
Klebsiella pneumoniae	0	0
Staphylococcus aureus	100	100
Accuracy	**75**	**75**

It has to be mentioned that the test evaluation dataset had more low-quality spectra in terms of signal-to-noise ratio (SNR) than the training cross-validation dataset (Figure S7). This could be another factor that influences the classification since small bands are lost due to the noise and cannot be considered by the model.

Due to the presence of a high number of bands in the PEI spectrum, the use of polynomial degrees higher than 1 for the wavenumber calibration can be justified. Analysis was repeated using a polynomial degree of 2 and 3, however, no improvement in accuracy could be detected (data not shown).

4. Discussion

The present study shows that in deep-UVRR not all polymers with an appropriate chemical structure are suitable to be used as calibration agents since their spectra do not show clearly defined, sharp bands within the entire spectral region. The overtime changes of the device significantly influence the band positions in the spectra and wavenumber calibration is required to ensure overtime comparable spectra and high data quality. Classification models after test evaluation with an independent dataset measured after 4 months performed best in classifying bacterial species when PET and Teflon were used for calibration, yielding an accuracy for differentiation of 76.8 and 75.6 % respectively. With these two polymers, all spectra of the Gram-positive isolates were correctly classified. With PEI and PS, the majority of the spectra from Gram-positive isolates could be correctly classified allowing to overcome misclassification by applying majority voting. None of the polymers could ensure differentiation between *Escherichia coli* and *Klebsiella pneumoniae* in the test data, indicating that wavenumber calibration alone is not enough to standardize the model's performance in differentiating close related and highly similar *Enterobacteriaceae* species when the database was established during a longer time period.

During wavenumber calibration, the wavenumber axis of the recorded spectra is modified by fitting to the Lorentzian Raman peaks of the standard substance using a fifth-order polynomial [25]. This procedure in spectra pre-processing "corrects" the Raman setup-dependent shift in the wavenumber axis according to the standard substance. However, the setup-dependent shifts are also present in the spectra of the standard substances. Thus, before performing the calibration of the bacteria spectra, the spectra of the standard substances also need to be adjusted to a "reference peak position" of high precision. In the present study, this was performed by obtaining spectra of the polymers with FT-Raman using a spectral resolution below 1 cm^{-1}. This resulted in high precision in the band positions of the polymers and since most of the peaks are present in both techniques, deep-UVRR and FT-Raman, the FT-Raman spectra could be used as reference standards for the polymer spectra measured with deep-UVRR.

It is interesting to observe that even when no calibration is performed in the training cross-validation dataset an almost perfect

differentiation of the isolates could be performed, even in the highly similar *Enterobacteriaceae* species. However, after evaluation with an independent dataset obtained after 4 months, the differentiation within both the Gram-positive and the Gram-negative groups was lost, and the model was only capable of discriminating the groups themselves. This shows that the overtime changes in the Raman setup were minor in the dataset obtained within a short time period but major after 4 months had passed, indicating the necessity of performing wavenumber calibration as a standard preprocessing step.

After wavenumber calibration with the different polymers and test evaluation the performance of the different models in differentiating the Gram-positive species varied. None of the *Staphylococcus aureus* spectra was classified incorrectly when calibrating with all polymers. Also, all *Enterococcus faecalis* spectra were correctly classified when calibrating whit PET and Teflon. When PEI and PS were used as calibration agents, misclassifications occurred but, the majority of the *Enterococcus faecalis* spectra were classified correctly allowing correct classification of the species after the application of majority voting. This indicates the importance of selecting the most suitable agent for wavenumber calibration since it can significantly influence the performance of the classification model, especially after test evaluation with an independent dataset after some time.

Due to the high similarities in the genome and cell biochemistry [26–28], the *Enterobacteriaceae* species are difficult to differentiate, sometimes even with the conventional techniques that are currently used in microbiology laboratories [29]. Raman spectra are superpositions of vibrations from many different cell components simultaneously and it is challenging to reveal such fine interspecies differences as present in the *Enterobacteriaceae* group. In previous Raman studies using excitation wavelengths in the visible range, it has been concluded that *Enterobacteriaceae* are difficult to classify [30] or even classified the *Enterobacteriaceae* as one group, incapable to differentiate the individual species [31,32].

In deep-UVRR, the selective enhancement of the Raman signals of the aromatic compounds in the bacterial macromolecules allows to focus on the difference in genotype, gene expression and protein composition and thus, the areas with the major interspecies differences are selectively analyzed. Simultaneously, the information deriving from interspecies similarities are excluded, due to the suppression of the Raman bands deriving from lipids and carbohydrates, improving the performance of the classification model. It has been previously shown that deep-UVRR could differentiate clinical *Klebsiella* spp. and *Escherichia coli* isolates with an accuracy of 92 % and *Klebsiella pneumoniae* from *Klebsiella oxytoca* with an accuracy of 90 % [20]. In the present study, it is shown that deep-UVRR can differentiate *Escherichia coli* from *Klebsiella pneumoniae* clinical isolates independent of the polymer used for wavenumber calibration. However, this ability is lost when test evaluation is performed with an independent dataset that was obtained after 4 months. The reasons for this phenomenon are most likely related to the overtime changes of the Raman setup that influenced the spectral quality more than the wavenumber calibration could correct. Another factor that could have influenced the classification results is the decreased SNR in the test evaluation dataset. Changes in the SNR can be related to the sample or the Raman setup. It can be influenced by factors such as the intensity of the laser or the laser light that reaches the objective and concerning the sample, by factors such as lower biomass or higher photodegradation. These parameters are highly affected by external factors as are changes in temperature and humidity and can be only controlled to a certain extent.

The overtime changes in the Raman setups are highly dependent on the measurement conditions and are influenced by variable factors such as temperature or changes in the laser's intensity and wavelength, that do not follow a systematic and predictable pattern. In this context, the influence on the spectra by the Raman setup itself also varies, affecting their reproducibility at an intrasample as well as the interlaboratory level that cannot be completely addressed and overcome so far. This is a major issue in the attempt to standardize Raman spectroscopy and develop this technique for clinical application and a large effort is required to understand this phenomenon and develop strategies to conquer it [33]. Wavenumber calibration is important for the model stability over time, but additional intensity calibration could help preprocess stability. Although this is challenging since for intensity calibration a continuous light source is required that produces a broad band in the UV region of interest and, to our knowledge, this does not exist so far for the deep-UV. However, in the present study it is shown that despite all the above-mentioned issues and just by adjusting the wavenumber calibration standard, the high sensitivity of deep-UVRR only fails in discriminating the very fine differences between the species of the *Enterobacteriaceae* group when test evaluated after 4 months. This shows that once the standardization of the method is achieved the application of Raman spectroscopy in clinical diagnostics can be a game changer since, the high sensitivity and speed combined with the low cost of this technique has all the requirements to improve patient care, health care finances as well as overall managing of infectious disease.

5. Conclusion

The present study highlights the necessity for performing wavenumber calibration as well as the importance of selecting the most suitable substance for wavenumber calibration in deep-UVRR to obtain the best possible classification of clinically relevant bacteria species. Calibration with PET and Teflon provided the best results since it allowed all spectra of the Gram-positive isolates to be correctly classified after test evaluation. PEI and PS performed less good however, the impact of misclassifications could still be limited by the application of majority voting. The highly accurate differentiation of the two *Enterobacteriacae* species in the training models, as provided by all used polymers, was lost after test evaluation. This strongly indicates that, despite wavenumber calibration, also other factors influence the spectral quality that need to be understood and addressed. The present study is an important step for the standardization of deep-UVRR and its development for clinical application.

Authors contribution

AP designed experiments, performed measurements, analyzed the data and wrote the manuscript; OR and TB discussed experiments, analyzed the data and drafted the manuscript; PR designed experiments and drafted the manuscript; JP provided material and instruments discussed experiments and drafted the manuscript. All authors have read and agreed to the published version of the manuscript.

Funding

This work is supported by the BMBF, in the project CarbaTech (FKZ 01EI1701) and the funding program Photonics Research Germany (FKZ 13 N15466 and 13 N15708) and is integrated into the Leibniz Center for Photonics in Infection Research (LPI). The LPI initiated by Leibniz-IPHT, Leibniz-HKI, UKJ and FSU Jena is part of the BMBF national roadmap for research infrastructures.

CRediT authorship contribution statement

Conceptualisation: AP, OR, TB, PR, JP; data curation: AP, OR, TB, PR; formal analysis: AP, OR, TB; founding acquisition: PR, JP; investigation: AP; methodology: AP, OR, PR; project administration: PR, JP; resources: JP; software: OR, TB; supervision: PR, JP; validation: AP, OR, TB, PR; visualisation: AP; writing-original draft: AP, OR, TB, PR, JP; writing-review & editing: AP, OR, TB, PR, JP.

Declaration of Competing Interest

The authors declare that they have no known competing financial interests or personal relationships that could have appeared to influence the work reported in this paper.

Data availability

Data will be made available on request.

Acknowledgments

We would like to thank Darina Storozhuk for her contribution to the development and support of the Ramanmetrix software and Ralf Heinke and Nicolae Tarcea for their technical support on the UVRR device. In addition, we would like to thank Jörg Aschemann and the company Gebr. DOLLE GmbH for providing us with polymer samples.

Appendix A. Supplementary material

Supplementary data to this article can be found online at https://doi.org/10.1016/j.saa.2022.122062.

References

[1] D.F.M. Willemse-Erix, M.J. Scholtes-Timmerman, J.-W. Jachtenberg, W.B. van Leeuwen, D. Horst-Kreft, T.C. Bakker Schut, R.H. Deurenberg, G.J. Puppels, A. van Belkum, M.C. Vos, K. Maquelin, Optical fingerprinting in bacterial epidemiology: Raman spectroscopy as a real-time typing method, J Clin Microbiol 47 (3) (2009) 652–659.

[2] B. Lorenz, C. Wichmann, S. Stöckel, P. Rösch, J. Popp, Cultivation-Free Raman Spectroscopic Investigations of Bacteria, Trends Microbiol. 25 (2017) 413–424, https://doi.org/10.1016/j.tim.2017.01.002.

[3] S. Pahlow, S. Meisel, D. Cialla-May, K. Weber, P. Rösch, J. Popp, Isolation and identification of bacteria by means of Raman spectroscopy, Adv Drug Deliv Rev 89 (2015) 105–120, https://doi.org/10.1016/j.addr.2015.04.006.

[4] S. Stöckel, J. Kirchhoff, U. Neugebauer, P. Rösch, J. Popp, The application of Raman spectroscopy for the detection and identification of microorganisms, J. Raman Spectrosc. 47 (2016) 89–109, https://doi.org/10.1002/jrs.4844.

[5] A. Pistiki, S. Monecke, H. Shen, O. Ryabchykov, T.W. Bocklitz, P. Rösch, R. Ehricht, J. Popp, C.P. Andam, Comparison of Different Label-Free Raman Spectroscopy Approaches for the Discrimination of Clinical MRSA and MSSA Isolates, Microbiol. Spect. 10 (5) (2022), https://doi.org/10.1128/spectrum.00763-22.

[6] A. Nakar, A. Pistiki, O. Ryabchykov, T. Bocklitz, P. Rösch, J. Popp, Detection of multi-resistant clinical strains of E. coli with Raman spectroscopy, Anal. Bioanal. Chem. 414 (2022) 1481–1492, https://doi.org/10.1007/s00216-021-03800-y.

[7] H.M. Sapers, J. Razzell Hollis, R. Bhartia, L.W. Beegle, V.J. Orphan, J.P. Amend, The Cell and the Sum of Its Parts: Patterns of Complexity in Biosignatures as Revealed by Deep UV Raman Spectroscopy, Front. Microbiol. (2019) 10.

[8] A. Locke, S. Fitzgerald, A. Mahadevan-Jansen, Advances in Optical Detection of Human-Associated Pathogenic Bacteria, Molecules 25 (2020) 5256, https://doi.org/10.3390/molecules25225256.

[9] A. Walter, W. Schumacher, T. Bocklitz, M. Reinicke, P. Rösch, E. Kothe, J. Popp, From bulk to single-cell classification of the filamentous growing Streptomyces bacteria by means of Raman spectroscopy, Appl. Spectrosc. 65 (2011) 1116–1125, https://doi.org/10.1366/11-06329.

[10] R.M. Jarvis, R. Goodacre, Ultra-violet resonance Raman spectroscopy for the rapid discrimination of urinary tract infection bacteria, FEMS Microbiol. Lett. 232 (2004) 127–132, https://doi.org/10.1016/S0378-1097(04)00040-0.

[11] Administration, F.a.D. *Bioanalytical Method Validation Guidance for Industry*; 24 May 2018.

[12] Agency, E.M. *Guideline on bioanalytical method validation*; 21 July 2011.

[13] S. Guo, R. Heinke, S. Stöckel, P. Rösch, T. Bocklitz, J. Popp, Towards an improvement of model transferability for Raman spectroscopy in biological applications, Vib. Spectrosc. 91 (2017) 111–118, https://doi.org/10.1016/j.vibspec.2016.06.010.

[14] U. Neugebauer, U. Schmid, K. Baumann, U. Holzgrabe, W. Ziebuhr, S. Kozitskaya, W. Kiefer, M. Schmitt, J. Popp, Characterization of bacterial growth and the influence of antibiotics by means of UV resonance Raman spectroscopy, Biopolymers 82 (2006) 306–311, https://doi.org/10.1002/bip.20447.

[15] G. Azemtsop Matanfack, A. Pistiki, P. Rösch, J. Popp, Raman Stable Isotope Probing of Bacteria in Visible and Deep UV-Ranges, Life 11 (10) (2021) 1003.

[16] G. Azemtsop Matanfack, A. Pistiki, P. Rösch, J. Popp, Raman 18O-labeling of bacteria in visible and deep UV-ranges, J. Biophotonics 14 (2021) e202100013.

[17] E.C. López-Díez, R. Goodacre, Characterization of Microorganisms Using UV Resonance Raman Spectroscopy and Chemometrics, Anal. Chem. 76 (2004) 585–591, https://doi.org/10.1021/ac035110d.

[18] Q. Wu, W.H. Nelson, S. Elliot, J.F. Sperry, M. Feld, R. Dasari, R. Manoharan, Intensities of E. coli nucleic acid Raman spectra excited selectively from whole cells with 251-nm light, Anal. Chem. 72 (2000) 2981–2986, https://doi.org/10.1021/ac990932p.

[19] D.M. Sievert, P. Ricks, J.R. Edwards, A. Schneider, J. Patel, A. Srinivasan, A. Kallen, B. Limbago, S. Fridkin, Antimicrobial-resistant pathogens associated with healthcare-associated infections: summary of data reported to the National Healthcare Safety Network at the Centers for Disease Control and Prevention, 2009–2010, Infect Control Hosp. Epidemiol. 34 (1) (2013) 1–14.

[20] A. Nakar, A. Pistiki, O. Ryabchykov, T. Bocklitz, P. Rösch, J. Popp, Label-free differentiation of clinical E. coli and Klebsiella isolates with Raman spectroscopy, J. Biophotonics n/a, e202200005 (2022), https://doi.org/10.1002/jbio.202200005.

[21] S. Stöckel, S. Meisel, B. Lorenz, S. Kloß, S. Henk, S. Dees, E. Richter, S. Andres, M. Merker, I. Labugger, P. Rösch, J. Popp, Raman spectroscopic identification of Mycobacterium tuberculosis, J. Biophoton. 10 (5) (2017) 727–734.

[22] A. Nakar, A. Pistiki, O. Ryabchykov, T. Bocklitz, P. Rösch, J. Popp, Detection of multi-resistant clinical strains of E. coli with Raman spectroscopy, Anal. Bioanal. Chem. 414 (4) (2022) 1481–1492.

[23] Darina Storozhuk, O.R., Juergen Popp and Thomas Bocklitz. RAMANMETRIX: a delightful way to analyze Raman spectra. *arXiv:2201.0758* **2022**.

[24] O. Ryabchykov, T. Bocklitz, A. Ramoji, U. Neugebauer, M. Foerster, C. Kroegel, M. Bauer, M. Kiehntopf, J. Popp, Automatization of spike correction in Raman spectra of biological samples, Chemometrics and Intelligent Laboratory Systems 155 (2016) 1–6, https://doi.org/10.1016/j.chemolab.2016.03.024.

[25] T. Dörfer, T. Bocklitz, N. Tarcea, M. Schmitt, J. Popp, Checking and Improving Calibration of Raman Spectra using Chemometric Approaches, Z. Phys. Chem. 225 (2011) 753–764, https://doi.org/10.1524/zpch.2011.0077.

[26] W. Moussaoui, B. Jaulhac, A.M. Hoffmann, B. Ludes, M. Kostrzewa, P. Riegel, G. Prévost, Matrix-assisted laser desorption ionization time-of-flight mass spectrometry identifies 90% of bacteria directly from blood culture vials, Clin Microbiol Infect 16 (2010) 1631–1638, https://doi.org/10.1111/j.1469-0691.2010.03356.x.

[27] D. Jonas, B. Spitzmüller, F.D. Daschner, J. Verhoef, S. Brisse, Discrimination of Klebsiella pneumoniae and Klebsiella oxytoca phylogenetic groups and other Klebsiella species by use of amplified fragment length polymorphism, Res. Microbiol. 155 (2004) 17–23, https://doi.org/10.1016/j.resmic.2003.09.011.

[28] N. Kunapareddy, J. Grun, R. Lunsford, S. Nikitin, Z. Wang, D. Gillis, Multiwavelength Resonance Raman Characterization of the Effect of Growth Phase and Culture Medium on Bacteria, Appl Spectrosc 69 (2015) 966–971, https://doi.org/10.1366/14-07770.

[29] A.F.G. Rave, A.V. Kuss, G.H.S. Peil, S.R. Ladeira, J.P.V. Villarreal, P.S. Nascente, Biochemical identification techniques and antibiotic susceptibility profile of lipolytic ambiental bacteria from effluents, Braz J Biol 79 (2019) 555–565, https://doi.org/10.1590/1519-6984.05616.

[30] I. Espagnon, D. Ostrovskii, R. Mathey, M. Dupoy, P.L. Joly, A. Novelli-Rousseau, F. Pinston, O. Gal, F. Mallard, D.F. Leroux, Direct identification of clinically relevant bacterial and yeast microcolonies and macrocolonies on solid culture media by Raman spectroscopy, J. Biomed. Opt. 19 (2014), https://doi.org/10.1117/1.jbo.19.2.027004, 027004-027004.

[31] S. Kloß, P. Rösch, W. Pfister, M. Kiehntopf, J. Popp, Toward Culture-Free Raman Spectroscopic Identification of Pathogens in Ascitic Fluid, Anal. Chem. 87 (2015) 937–943, https://doi.org/10.1021/ac503373r.

[32] C.-S. Ho, N. Jean, C.A. Hogan, L. Blackmon, S.S. Jeffrey, M. Holodniy, N. Banaei, A. A.E. Saleh, S. Ermon, J. Dionne, Rapid identification of pathogenic bacteria using Raman spectroscopy and deep learning, Nat. Commun. 10 (2019) 4927, https://doi.org/10.1038/s41467-019-12898-9.

[33] S. Guo, C. Beleites, U. Neugebauer, S. Abalde-Cela, N.K. Afseth, F. Alsamad, S. Anand, C. Araujo-Andrade, S. Aškrabić, E. Avci, M. Baia, M. Baranska, E. Baria, L.A.E. Batista de Carvalho, P. de Bettignies, A. Bonifacio, F. Bonnier, E.M. Brauchle, H.J. Byrne, I. Chourpa, R. Cicchi, F. Cuisinier, M. Culha, M. Dahms, C. David, L. Duponchel, S. Duraipandian, S.F. El-Mashtoly, D.I. Ellis, G. Eppe, G. Falgayrac, O. Gamulin, B. Gardner, P. Gardner, K. Gerwert, E.J. Giamarellos-Bourboulis, S. Gizurarson, M. Gnyba, R. Goodacre, P. Grysan, O. Guntinas-Lichius, H. Helgadottir, V.M. Grošev, C. Kendall, R. Kiselev, M. Kölbach, C. Krafft, S. Krishnamoorthy, P. Kubryck, B. Lendl, P. Loza-Alvarez, F.M. Lyng, S. Machill, C. Malherbe, M. Marro, M.P.M. Marques, E. Matuszyk, C.F. Morasso, M. Moreau, H. Muhamadali, V. Mussi, I. Notingher, M.Z. Pacia, F.S. Pavone, G. Penel, D. Petersen, O. Piot, J.V. Rau, M. Richter, M.K. Rybarczyk, H. Salehi, K. Schenke-Layland, S. Schlücker, M. Schosserer, K. Schütze, V. Sergo, F. Sinjab, J. Smulko, G. D. Sockalingum, C. Stiebing, N. Stone, V. Untereiner, R. Vanna, K. Wieland, J. Popp, T. Bocklitz, Comparability of Raman Spectroscopic Configurations: A Large Scale Cross-Laboratory Study, Anal. Chem. 92 (24) (2020) 15745–15756.